Al-Rafidain Journal of Engineering Sciences

Journal homepage https://rjes.iq/index.php/rjes

ISSN 3005-3153 (Online)

Oscillating Heat Pipe Start-up and Flow Characteristics with Water as Working Fluid

Mohammed H. Taher [1*], Wail S. Wadee [2]

[1,2] Mechanical Engineering Department, College of Engineering, Baghdad University, Baghdad, Iraq.

ARTICLE INFO

Article history:

Received	31 August 2024
Revised	01 September 2024
Accepted	06 September 2024
Available online	08 September 2024

Keywords:

Oscillating heat pipe,

Oscillating movement,

Pulsating heat pipe,

Start-up,

Two-phase flow.

ABSTRACT

Thermal management has grown more and more problematic as electronic components continue to get faster and smaller. One of the passive two-phase cooling systems are Oscillating heat pipe (OHP) that have the capacity to transmit a significant quantity of thermal energy across long distances. Oscillating heat pipe is a device that has the potential to satisfy this developing requirement. An investigation into the effects of orientation, filling ratio, and heat load on the initiation and characteristics of oscillatory motion, combining numerical simulations with experimental validation. A copper tube with a 2 mm inner diameter and a 2 mm wall thickness is used to fabricate the OHP. The condenser, evaporator, and adiabatic sections are designed with lengths of 50 mm, 50 mm, and 150 mm, respectively. Results showed that the onset of oscillation occurs more rapidly with increasing input heat flux values compared to lower heat input conditions. The amplitude variations of the temperature of evaporator raised with the raising of heating power. The curves for the higher heat inputs (60 and 80 watts) appear to have higher average evaporator temperatures throughout the test compared to the 40-watt curve. Oscillation movement in tubes is proportional to charge ratio, and it is observed that it rises as charge ratio increases. It demonstrates that in Closed-loop oscillating heat pipe, a sufficient charge ratio is required to maintain the motion of oscillation.

Symbols list

Symbols	Description	Acronym List
T	Temperature [°C]	CFD – Computational fluid dynamics
ΔT	Temperature difference [°C]	CLOHP – Closed loop oscillating heat pipe
Subscripts		HP – Heat Pipes
a	adiabatic	OHP – Oscillating Heat Pipe
c	Condenser	PHP – Pulsating Heat Pipe
e	Evaporator	VOF – Volume of Fluid

* Corresponding author E-mail address: mohammed.taher2103m@coeng.uobaghdad.edu.iq

https://doi.org/10.61268/b9zs0s73

1. Introduction

Heat pipes have found extensive application in diverse systems owing to their exceptional thermal management capabilitiesKearney, et al. [1], Dang, et al. [2]. Thermal management challenges have extended beyond the electronics industry, becoming prevalent in diverse engineering systems and their components Agostini, et al. [3], Olivier, et al. [4]. Conventional heat pipes (CHP) may not provide optimal thermal management owing to limitation like as sonic, boiling, and capillary limitations Roth, et al. [5]. Furthermore, one of the factors contributing to CHP's declining market share is the comparatively expensive cost of construction Grover, et al. [6]. The oscillating heat pipe (OHP), first introduced by Akachi in the 1990s Akachi [7], has emerged as a promising solution for efficient heat transfer, capturing the interest of numerous researchers. The OHP has demonstrated significant potential as a result of its outstanding characteristics such as compact structure, excellent heat transfer performance, rapid thermal response, and independence from external power sources Qu, et al. [8]. The oscillating heat pipe has shown great promise for applications in waste heat recovery Zhao, et al. [9], solar energy utilization Jin, et al. [10], electronic cooling devices Wang, et al. [11], batteries for electric vehicles Wei, et al. [12], and the Heat-exchanging devices Jafari Mosleh, et al. [13], etc. Its advantages include simple construction, miniaturization capability, high heat transfer capacity, flexibility, and low cost Liu, et al. [14]. There are various types of OHP : closed loop, closed end, closed loop with check valve, and open loop. The most effective type of OHP, according to numerous earlier studies, is the oscillating-heat pipe type closed-loop Hai [15]. The capillary tube, featuring multiple bends, forms the basis of an oscillating heat pipe. It is divided into three sections: an evaporator, an adiabatic section, and a condenser Khandekar and Groll [16]. The tube is initially evacuated and partially filled with working fluid before the heat load is applied. The heat absorbed during evaporation is transferred to the condenser via two-phase flow, involving bubble, slug, and annular flow patterns, which contribute to both latent and sensible heat transfer Bastakoti, et al. [17]. The alternating phases of evaporation and condensation generate a non- uniform pressure field within the OHP, resulting in an oscillatory motion of the working fluid. The oscillatory motion significantly enhances convective heat transfer within the OHP, contributing to its efficient thermal performance.

In-depth studies of the OHP have been carried out, exploring its performance under various operating conditions and configurations. Xian, et al. [18] investigation into the influence of working fluid on OHP heat transfer characteristics revealed that water-based OHPs consistently outperformed ethanol-based OHPs in terms of overall performance and stability. Ji, et al. [19] discovered that superhydrophobic surfaces can induce oscillatory motion in OHPs, enabling their operation in a manner distinct from traditional wicked heat pipes. However, superhydrophobic OHPs exhibit a higher thermal resistance compared to those with hydrophilic inner surfaces. Lin, et al. [20] findings suggest that for vertical, four-turn, water-based OHPs, an inner diameter greater than 0.8 mm is necessary to achieve optimal heat transfer performance. Chien, et al. [21] conducted CLOHPs with non-uniform channels exhibited enhanced thermal performance and maintained functionality at all orientations, particularly at higher filling ratios. Patel, et al. [22] findings demonstrated that modifying the surface tension of OHP working fluids through the addition of pure fluids or surfactants can significantly reduce the required start-up heat input, improving the system's efficiency. Nikolayev [23], Nekrashevych and Nikolayev [24] numerically investigated the influence of tube heat conduction on single and multi-turn OHP start-up. Their findings indicate that the temperature gradient along the tube is the primary factor influencing the start-up threshold. Moreover, bubble generation was found to be essential for maintaining

oscillations in the presence of tube heat conduction. Xu, et al. [25] investigation into the heat-transfer performance of OHPs with hybrid working fluids revealed that a 30% ethanol-water mixture by volume exhibited the most effective thermal characteristics. Barrak, et al. [26] research revealed that incorporating OHPs as heat exchangers in air-conditioning systems can substantially enhance the dehumidification capabilities of cooling coils. The study found that water, binary, and methanol working fluids led to dehumidification improvements of 17%, 21%, and 25%, respectively. Qu, et al. [27] study suggests that while increasing initial pressure can enhance heat transfer in OHPs, it also comes at the cost of increased thermal resistance, which may impact overall efficiency. Mehta, et al. [28] CLFP-OHP model compared the effects of various operational and morphological factors. Among the tested configurations, acetone in a vertical orientation with square channels (2x2 mm) at a filling ratio of 60% exhibited the highest performance. Kammuang-lue, et al. [29], Li, et al. [30] revealed a direct correlation between adiabatic section length and CLPHP heat flow. While increasing adiabatic length initially enhances heat transfer, there exists a point of diminishing returns beyond which further increases become less beneficial. Siritan, et al. [31] demonstrated the potential of CLOHPs as a cost-effective alternative to thermosyphons in industrial evacuated tube solar water heater systems. The optimized CLOHP configuration, with a 1.50 mm inner diameter, a 1.25 m evaporator length, and four sets, achieved a total water collection rate of 518 W, leading to estimated net savings of $901.40 over ten years. Hammad [32] demonstrated the influence filling ratio, inclination angle, and input power on the thermal resistance of pulsating heat pipes. An optimal filling ratio range of 40-70% was identified for both isopropanol and distilled water. Additionally, increasing input power resulted in lower thermal resistance. Isopropanol consistently exhibited superior thermal performance compared to distilled water. Choi and Zhang [33] simulations demonstrated that the shape of OHPs significantly influences the initiation of circulation. Asymmetric OHPs were found to exhibit an earlier start-up compared to symmetric OHPs. The numerical simulations conducted by Vo, et al. [34], Wang, et al. [35], utilizing the VOF approach and CFD techniques, successfully validated the experimental observations of phase transition and heat transfer phenomena in the pulsating heat pipe.

This research comprehensively investigated the performance of oscillating heat pipes with a 2 mm inner diameter. Experiments were performed to evaluate the impact of filling-ratios, orientation, and power input on the start-up behavior, and flow patterns.

2. Experimental apparatus and methodology

A closed-loop OHP made of red-copper tubing with dimensions of 2 mm inner diameter and 4 mm outer diameter is used in this study. The OHP had a three-turn configuration, as shown in Figure 1. The condenser, evaporator, and adiabatic sections are designed with lengths of 50 mm, 50 mm, and 150 mm, respectively. It employed water as the working fluid at filling ratios of 50%, 60%, and 70%. Two flexible heaters attached to the evaporator section, as shown in Figure 2., supplied heat inputs of 40, 60, and 80 W. A 120-VAC variable output transformer controlled the power supply to the heaters. A water-cooling jacket maintained at 16°C used to cool the condenser section. The flow rate measurements of water have been done by utilizing glass rotor flowmeter type with range (25-250) ml/min. The cooling water flow rate, as measured by a flowmeter, is maintained at 100 ml/min. Temperature data was collected from thermocouples mounted on the exterior of the CLOHP to determine temperature distributions. Thermocouples were strategically located on the OHP to measure temperatures at various points. Four thermocouples were placed on the evaporator section (T_e), two in the middle of the adiabatic section (T_a), and four on the condenser section (T_c) as shown in Figure 3. A 12-channel thermocouple input data logger, model BTM-4208SD with an accuracy of ± 0.6°C, was used

to record the temperature readings from the thermocouples. Pressure variation tracked using a vacuum gauge capable of measuring pressure from -30 to 220 inHg. As part of the experimental setup, a DC 12V mini vacuum pump was employed to evacuate the air from the oscillating heat pipe. The experiment began by orienting the OHP to the desired angle. After evacuating the heat pipe, the working fluid was injected using a syringe to achieve the specified charging ratio. The tests commenced once the entire insulated test assembly reached thermal equilibrium with the circulating water. A constant ambient temperature of 25°C was maintained for all experiments.

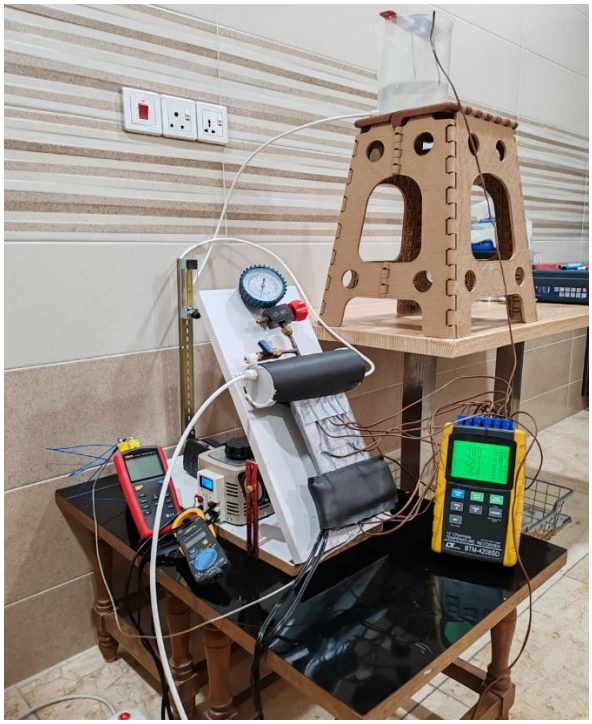

Figure 1: Test rig arrangement.

(a)

(b)

Figure 2: The flexible heaters attachment setup.

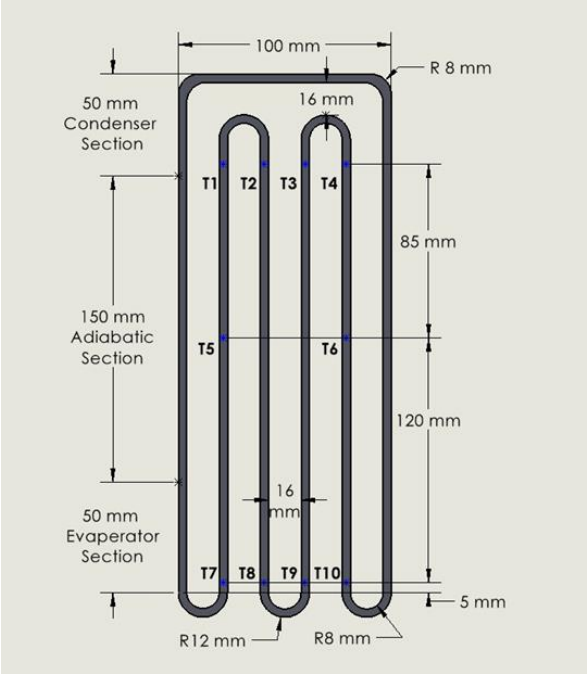

Figure 3: The arrangement of thermocouple nodes for measuring wall temperature.

3. Numerical Model

Computational fluid dynamics simulations carried out using ANSYS Fluent 2022/R1. The volume-of-fluid (VOF) model was adopted to model the interface between liquid and vapor phases in two-phase flow simulations. ANSYS Design-Modeler was employed to construct a 3D geometric model of the OHP for subsequent simulations. The computational domain was discretized into a mesh comprising 56,753 nodes and 8,248 elements, using an element size

of 148.8 mm in ANSYS Workbench as shown in Figure 4. The evaporator section was subjected to constant heat flux boundary conditions at power levels of 40, 60, and 80 W. A zero-heat flux boundary was imposed on the adiabatic section to simulate perfect insulation. The condenser was thermally maintained at a constant temperature of 293 K. An enhanced k-epsilon turbulence model, considering thermal effects and curvature correction, was employed.

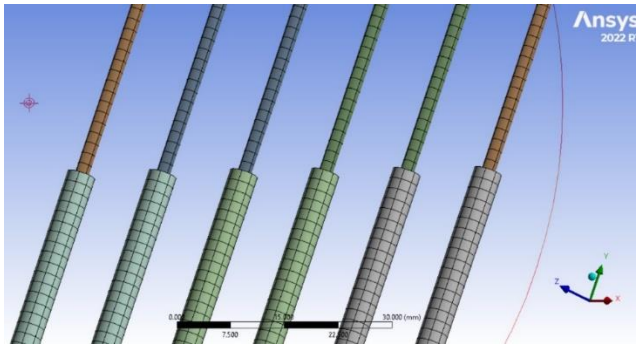

Figure 4: Mesh discretization.

4. Results and discussion

4.1 Experimental Results

4.1.1 Influence of charging-ratio on the temperature's variation at vertical position OHP under different heat-loads

The OHP condenser and evaporator's temperature time history, as captured by thermocouples mounted on the tube, is presented in Figure 5 to Figure 7**.** It shows that the fluctuation of the temperatures measured for heating powers 40, 60, and 80 W. Notably, these temperature oscillations were continuous, with the frequency increasing proportionally to the applied heat input. It can be seen that, for all cases, the oscillating heat pipe with the specified parameters reaches a steady oscillating state after an initial start-up period. The experimental data reveals that the average evaporator temperature for the higher heat input conditions (60 and 80 watt) exhibited a consistently elevated trend throughout the testing period compared to the 40-watt curve.

The evaporator and condenser section's temperature differences for heat-loads (40, 60, and 80W) are about (17, 22, and 28 ºC), receptively. It can be seen a higher filling ratio can lead to a higher evaporator temperature (ΔT increases) because there's less space for vapor to form and drive the heat transfer cycle. Conversely, a lower filling ratio might lead to a lower evaporator temperature (ΔT decreases), but if it's too low, it might not be enough to sustain a continuous cycle.

4.1.2 Influence of charging-ratio on the temperature's variation at 60º Inclined position OHP under different heat-loads

The Figures (8–10) shows the trend of average evaporator temperature across different filling ratios for a 60-degree orientation at various heat input. Experimental result shows the same outcomes of numerical tests that for all three filling ratios (50%, 60%, and 70%), the average evaporator temperature increases as the heat input increases. This is typically expected, as higher heat input increases the energy available to the evaporator part, increasing its temperature.

The evaporator and condenser section's temperature differences at heat-loads 40, 60, and 80 W are about (20, 28 and 31 ºC), receptively.

4.1.3 Influence of charging-ratio on the temperature's variation at 30º Inclined position OHP under different heat-loads

The Figures (11–13) presents the results obtained for the evaporator and condenser temperatures experimentally at each filling ratio for a 30-degree orientation at various heat input. Experimental result shows similar behavior of numerical tests that at 70% charged ratio results a larger volume of working fluid which leave less space for vapor formation and pressure fluctuations necessary for efficient oscillation. A larger fluid mass required more energy to overcome inertia and initiate/maintain stable oscillations. It observed that a 50% or 60% filling ratio might be optimal for achieving stable oscillation in this specific 30° inclined OHP with water as the working fluid. That lower charging-ratios (50%

and 60%), These filling ratios provide a good balance between enough liquid is available for efficient heat transfer and initial pressure generation, and There's sufficient space for vapor formation and pressure fluctuations to drive stable oscillations.

The evaporator and condenser section's temperature differences at heat-loads 40, 60, and 80 W are about (23, 38 and 41 ºC), receptively.

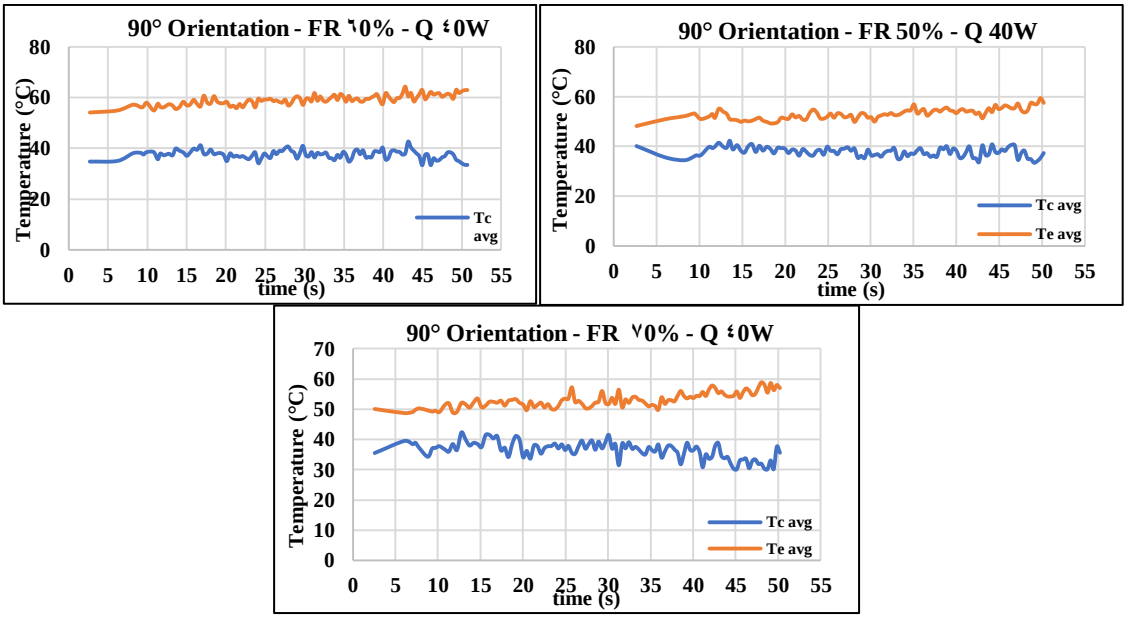

Figure 5: Temperatures variation at vertical position, for different charging ratios at 40 W heat-load after reaches steady-condition.

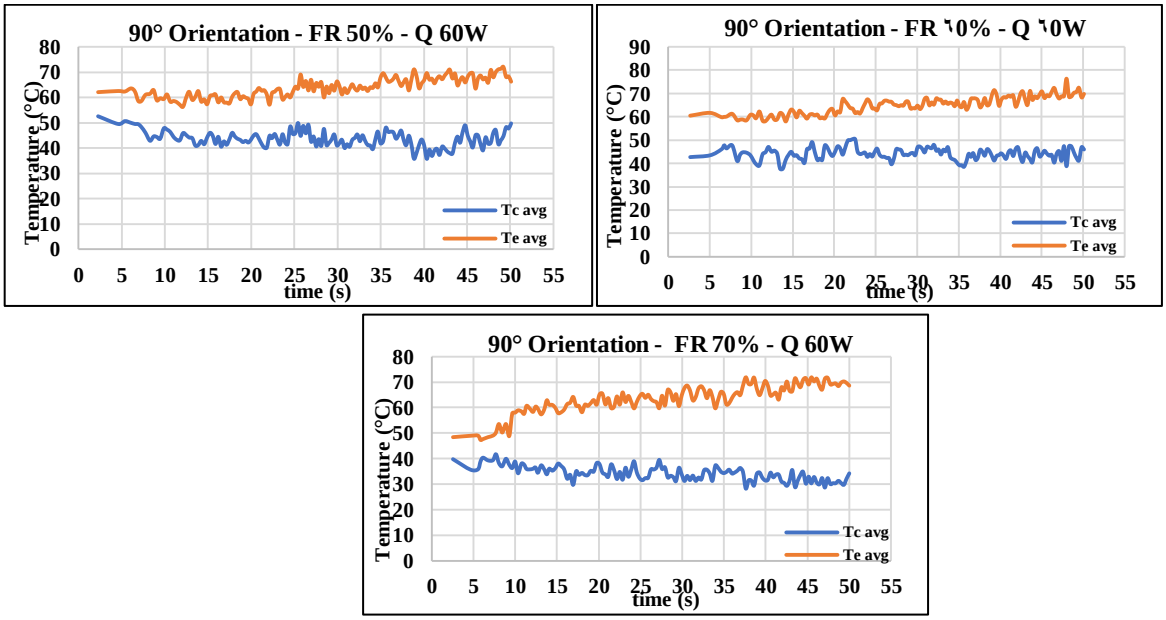

Figure 6: Temperatures variation at vertical position, for different charging ratios at 60 W heat-load after reaches steady-condition.

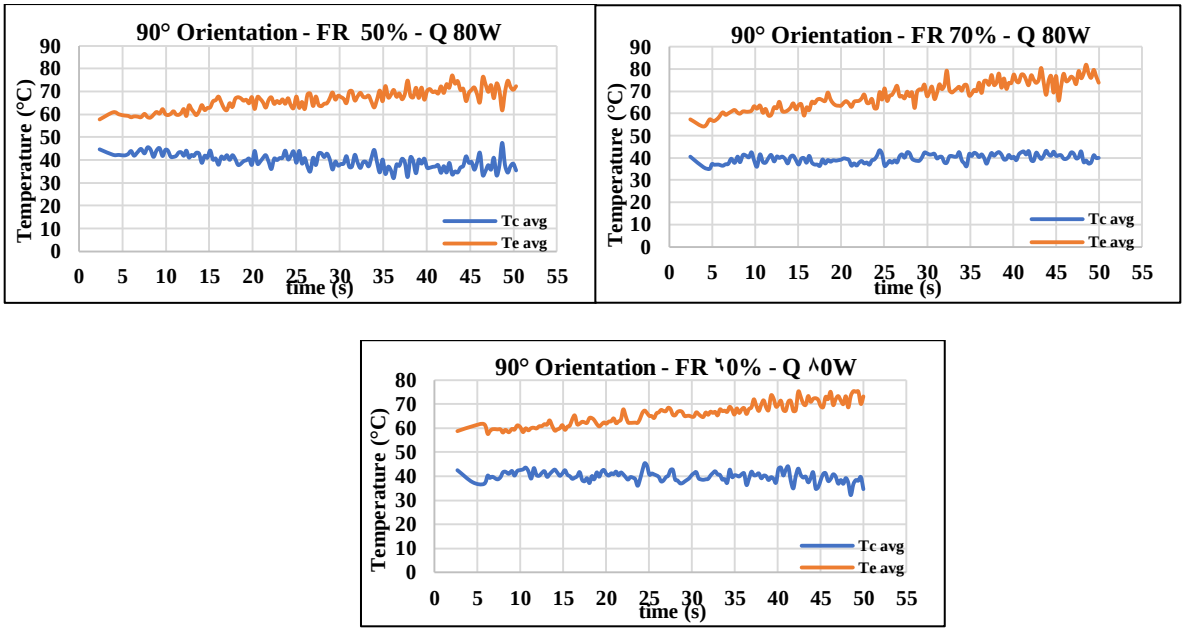

Figure 7: Temperatures variation at vertical position, for different charging ratios at 80 W heat-load after reaches steady-condition.

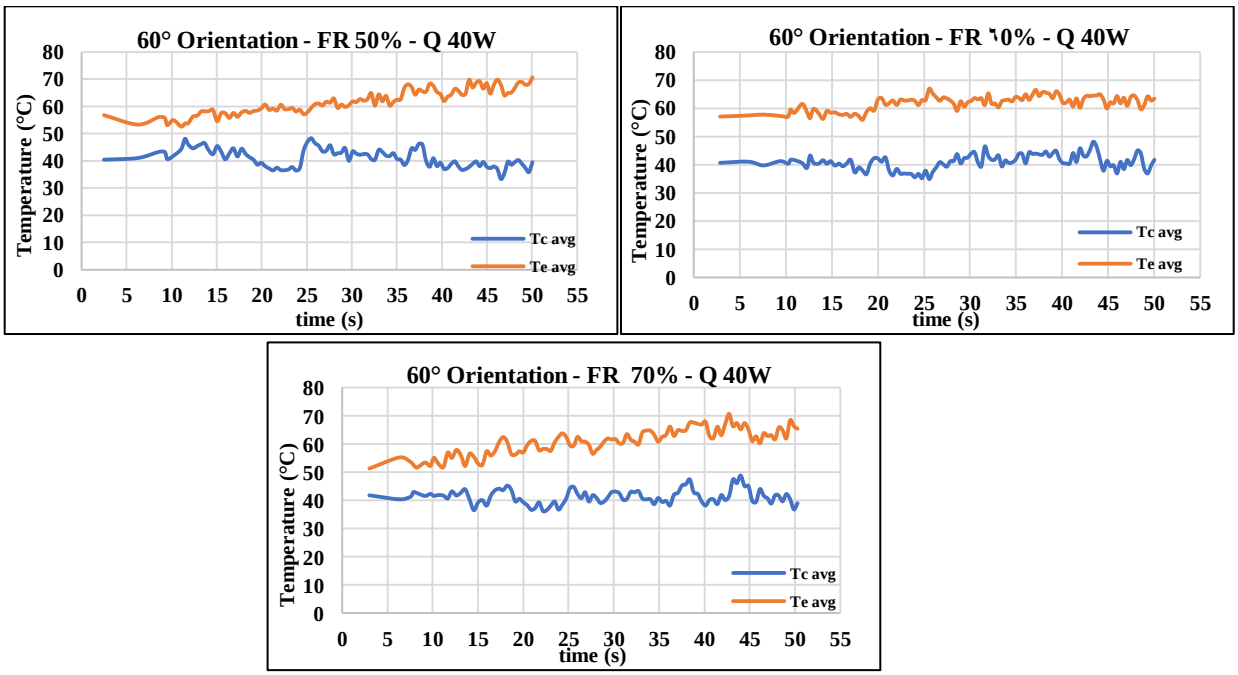

Figure 8: Temperatures variation for 60° orientation, for different charging ratios at 40 W heat-load after reaches steady-condition.

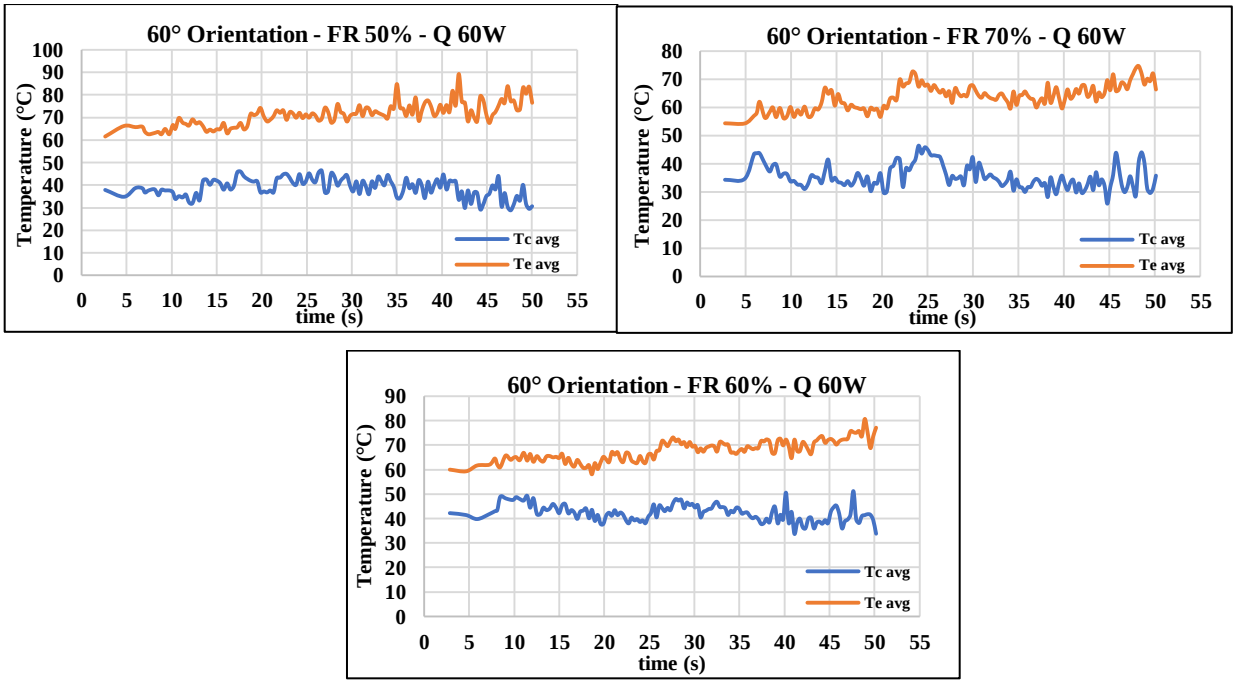

Figure 9: Temperatures variation for 60° orientation, for different charging ratios at 60 W heat-load after reaches steady-condition.

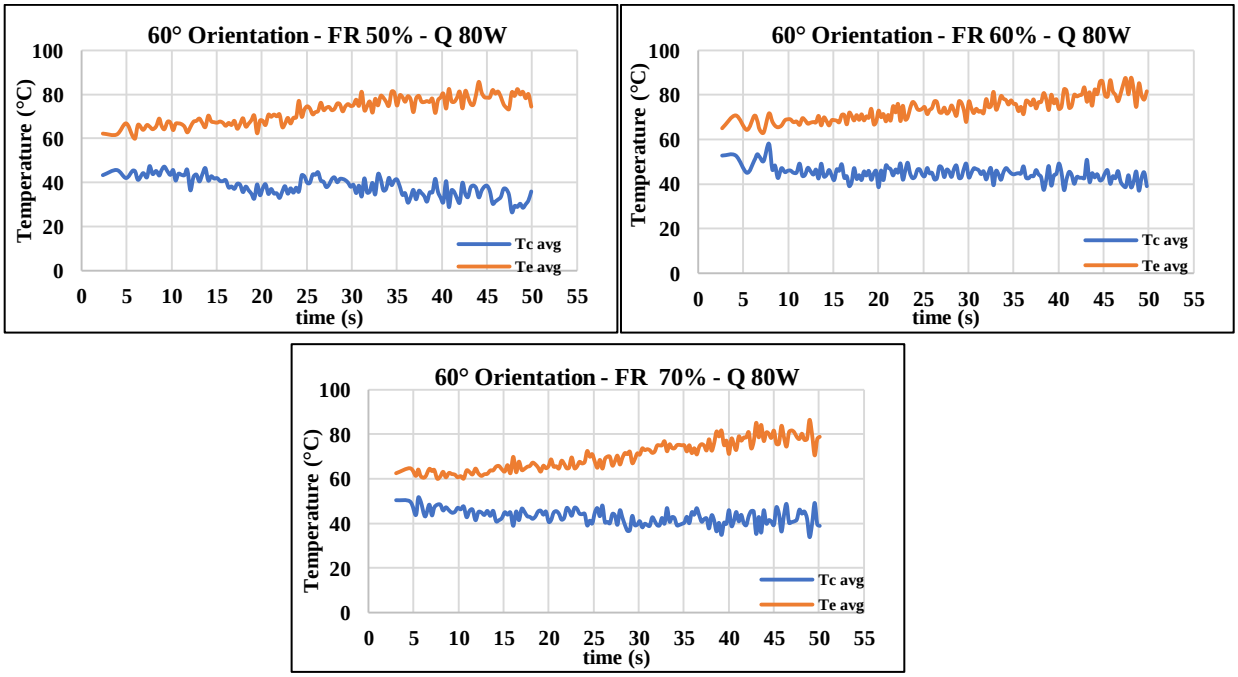

Figure 10: Temperatures variation for 60° orientation, for different charging ratios at 80 W heat-load after reaches steady-condition.

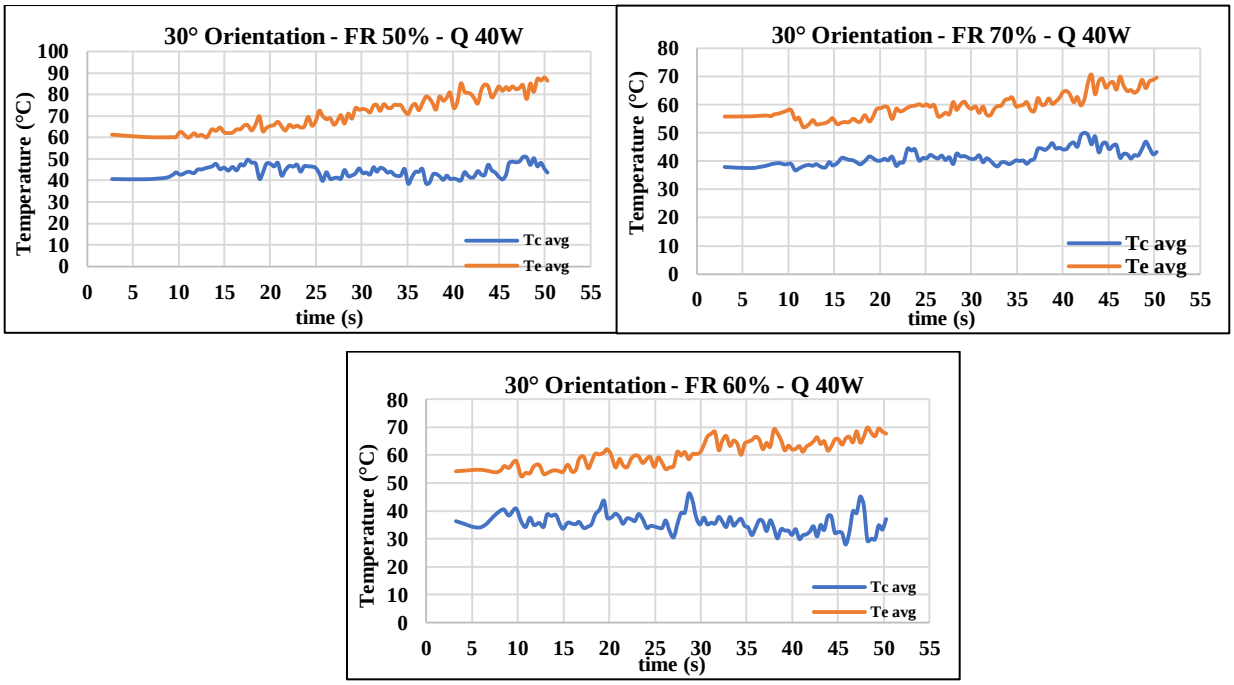

Figure 11: Temperatures variation for 30° orientation, for different charging ratios at 40 W heat-load after reaches steady-condition.

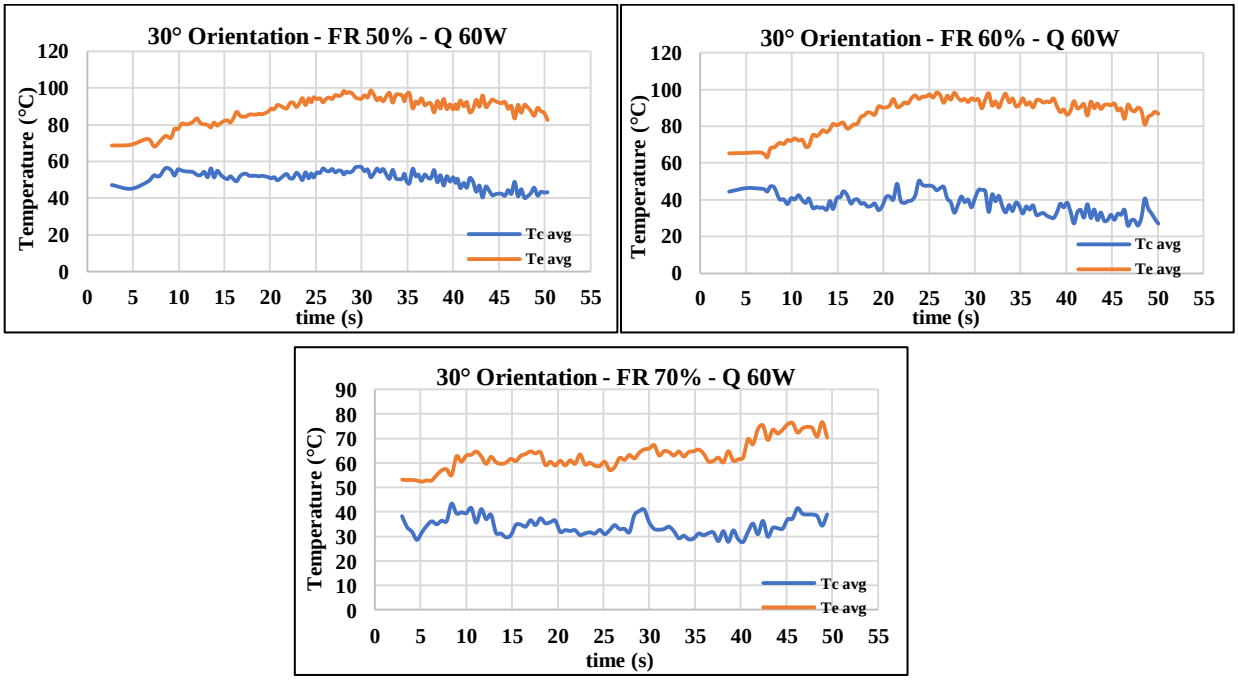

Figure 12: Temperatures variation for 30° orientation, for different charging ratios at 60 W heat-load after reaches steady-condition.

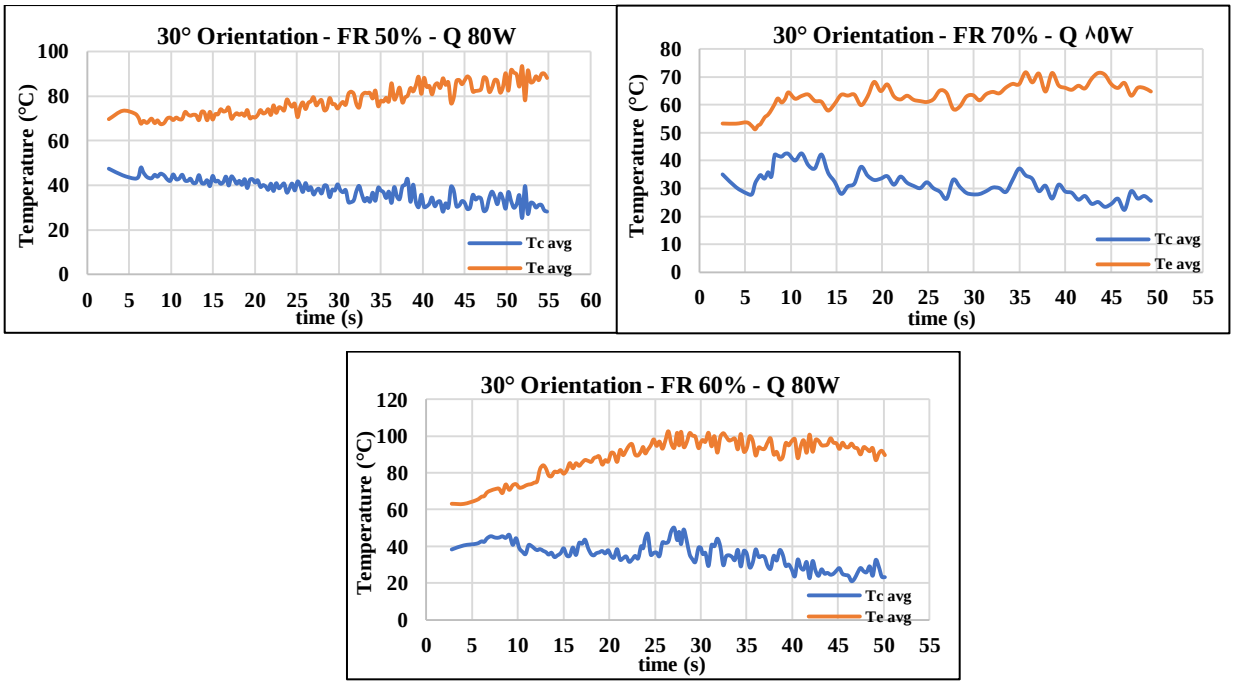

Figure 13: Temperatures variation for 30° orientation, for different charging ratios at 80 W heat-load after reaches steady-condition.

*4.2 **Numerical Results***

4.2.1 Influence of charging-ratio on the temperature of evaporator and condenser at vertical position OHP under different heat-loads.

As mentioned in the earlier section, the OHP form a closed system with 3-turn and 2 mm inner diameter is numerically tests for various operating conditions. Figures (14 –16) shows the temperature time history for tests for various filling ratios and heating powers. It can observe that both the evaporator and condenser temperatures fluctuate over time, which is a characteristic of an oscillating heat-pipe. The operating fluid (water in this case) evaporates

in the hotter evaporator part, creating vapor-bubbles that travel to the cooler condenser section. Due to pressure variations, vapor bubbles will condense and flow to the evaporator when they reach the condenser. This cycle of evaporation and condensation causes the temperatures in the evaporator and condenser to fluctuate. It is observed the amplitude variations of the temperature of evaporator raised with the raising of heating power. The curves for the higher heat inputs (60 and 80 watts) appear to have higher average evaporator temperatures are about (58.6 and 70 ºC) throughout the test compared to the 40-watt curve that average evaporator temperature is 46.3 ºC. It is anticipated that an increase in heat input will result in an increase in energy and temperature in the evaporator portion.

The evaporator and condenser section's temperature differences are about 20ºC at 40W while at 60 and 80W heat input the difference are 25 and 31 ºC, receptively.

Test results show that there's a period of time before the motion of oscillation begins. This phenomenon can be attributed to the requirement of a sufficiently high vapor-pressure within the evaporator to displace the liquid-vapor plug interface. Additionally, the time taken for the OHP to reach its operational state is influenced by the heat input rate in the evaporator and the heat rejection rate in the condenser. The minimum time required for the initiation of oscillatory motion was observed to be 5 seconds at a power input of 80 Watts.

4.2.2 Influence of charging-ratio on the temperature of evaporator and condenser at 60º Inclined position OHP under different heat-loads.

The Figures (17–19) shows the trend of average evaporator and condenser temperatures across different filling ratios for a 60-degree orientation at various heat input. For all three filling ratios (50%, 60%, and 70%), the average evaporator temperature increases as the heat input increases. This is expected because more heat input adds more energy to the evaporator section, raising its temperature.

The oscillation motion of vapor-plugs and liquid-slugs within channels is primarily driven by pressure variations arising within the channel due to the interplay of (sensible) and (latent) heat transport mechanisms. Sensible heat transport involves the transfer of thermal energy between theliquid and vapor phases without a change in phase. This occurs due to the temperature difference between the two phases and the resulting heat flux. As the liquid-slug moves through the channel, it absorbs heat from the surrounding walls, causing its temperature to increase. This increase in temperature leads to a decrease in the liquid's density, which in turn contributes to the formation of vapor bubbles.

Latent heat transport involves the transfer of thermal energy during a phase change, such as the evaporation of liquid to vapor or the condensation of vapor to liquid. This process is accompanied by a significant change in volume, which further influences the oscillation motion. As the liquid slug moves through the channel, some of the liquid evaporates to form vapor bubbles, absorbing a large amount of latent heat in the process. This evaporation leads to a decrease in the liquid's volume and an increase in the vapor's volume, contributing to the overall pressure variations within the channel.

Oscillation movement in tubes is proportional to charge ratio, and it is observed that it rises as charge ratio increases. It is discovered that at high charge ratios, there is a greater oscillation movement of vapor plugs and liquid slugs in the OHP. It demonstrates that in CL-OHP, a sufficient charge ratio is required to maintain the motion of oscillation.

The evaporator and condenser section's temperature differences at heat-load 40 W is around 23 ºC, while at 60 and 80 W are about (35 and 39 ºC), receptively.

4.2.3 Influence of charging-ratio on the temperature of evaporator and condenser at 30º Inclined position OHP under different heat-loads.

The Figures (20–22) describes the results obtained for the evaporator and condenser temperatures at each filling ratio for a 30-degree orientation at various heat input. It’s found at lower filling ratio (50%) with less working fluid, the evaporator might reach its saturation temperature faster, potentially leading to a slightly lower average evaporator temperature compared to higher filling-ratio. It shows that the inclined angle of OHP can influence both amplitude and frequency of these temperature-oscillations. It is discovered that at low charge ratios, there is a greater oscillation movement of vapor plugs and liquid slugs in the OHP. At a 30° inclination, the gravitational force acting on the working fluid is less effective compared to a vertical OHP. This means gravity plays a smaller role in driving the movement of bubbles and liquid slugs within the pipe. Pressure forces driven by temperature differences and surface tension become the dominant factors governing bubble and slug movement. The interplay between pressure forces and surface tension can determine the amplitude and frequency of the oscillations within the OHP.

The evaporator and condenser section's temperature differences at heat-loads 40, 60, and 80 W are about (26, 41 and 49 ºC), receptively.

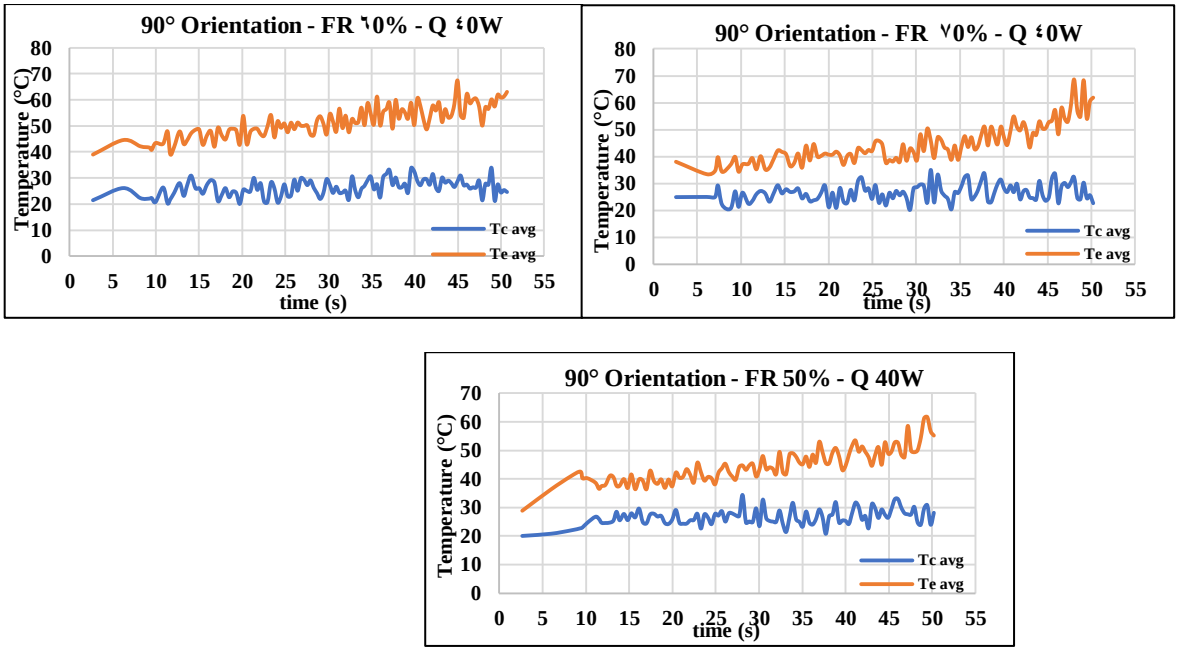

Figure 14: Numerically temperature variation in 90°orientation, for different charging ratios at 40 W heat-load after reaches steady-condition.

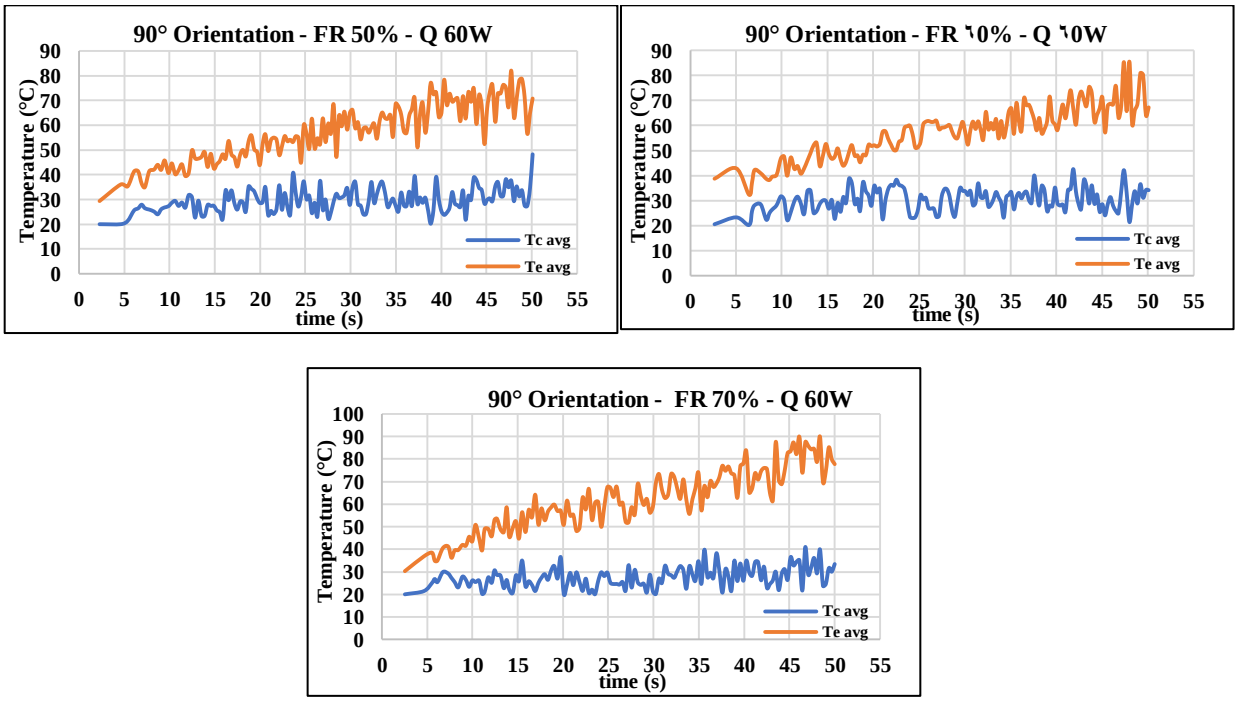

Figure 15: Numerically temperature variation in 90°orientation, for different charging ratios at 60 W heat-load after reaches steady-condition.

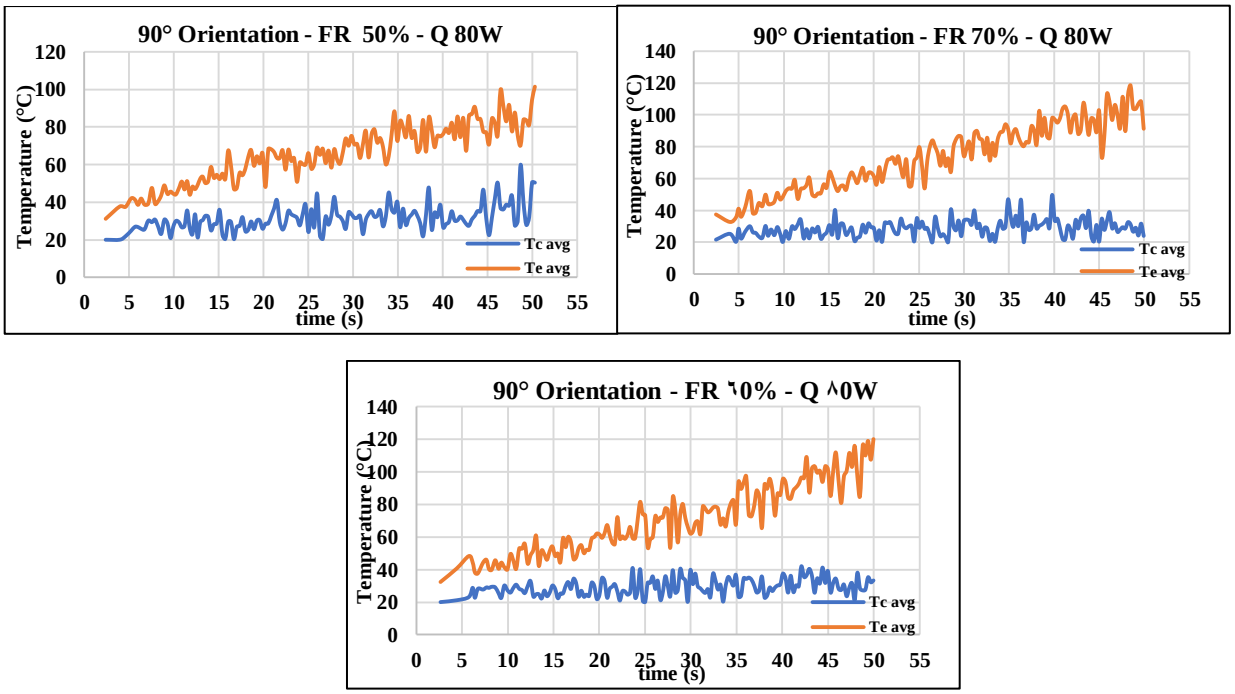

Figure 16: Numerically temperature variation in 90°orientation, for different charging ratios at 80 W heat-load after reaches steady-condition.

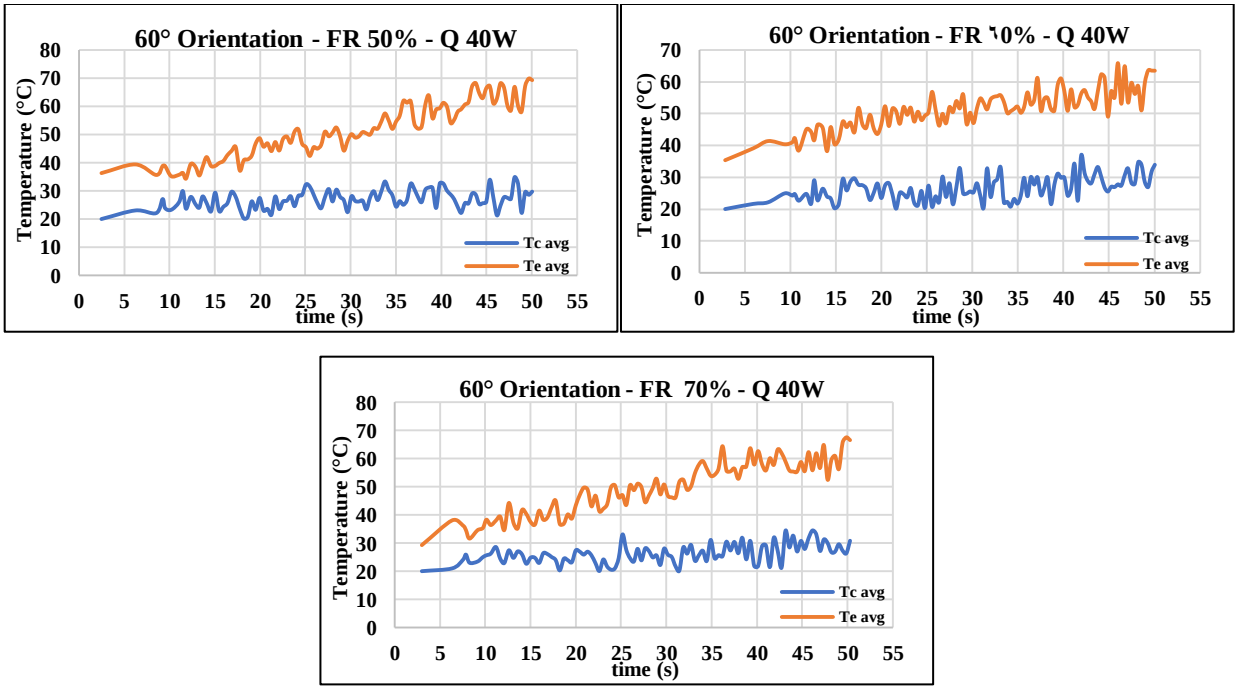

Figure 17: Numerically temperature variation in 60°orientation, for different charging ratios at 40 W heat-load after reaches steady-condition.

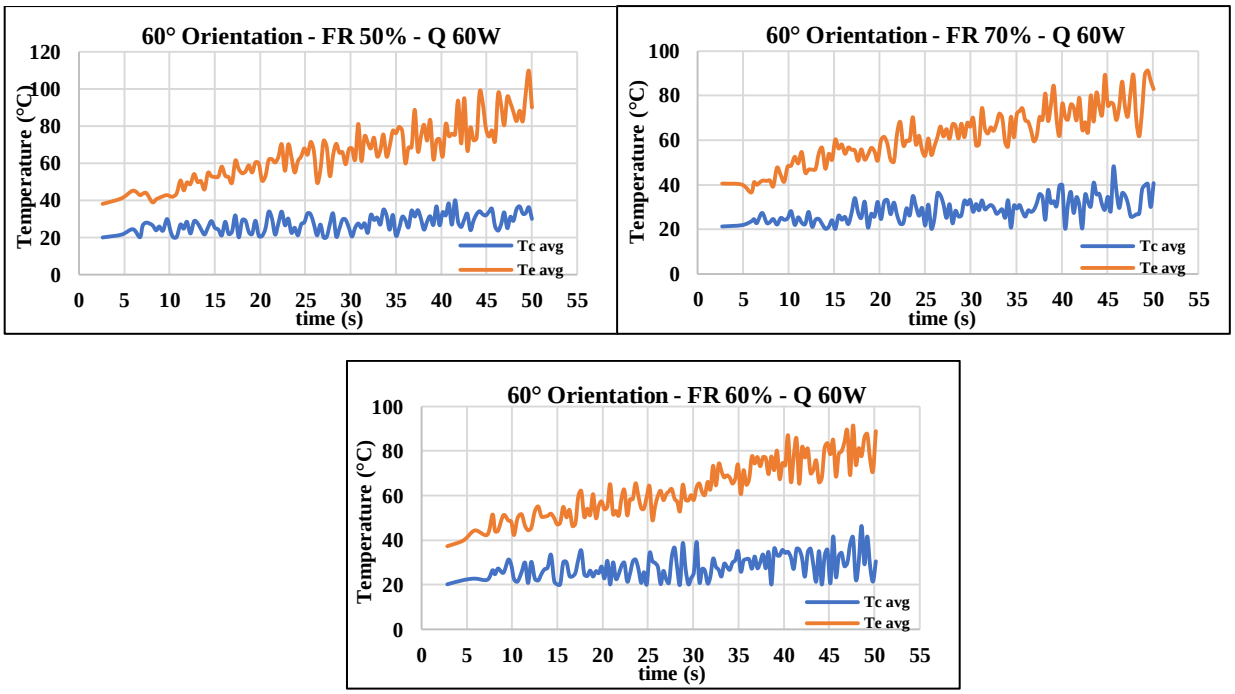

Figure 18: Numerically temperature variation in 60°orientation, for different charging ratios at 60 W heat-load after reaches steady-condition.

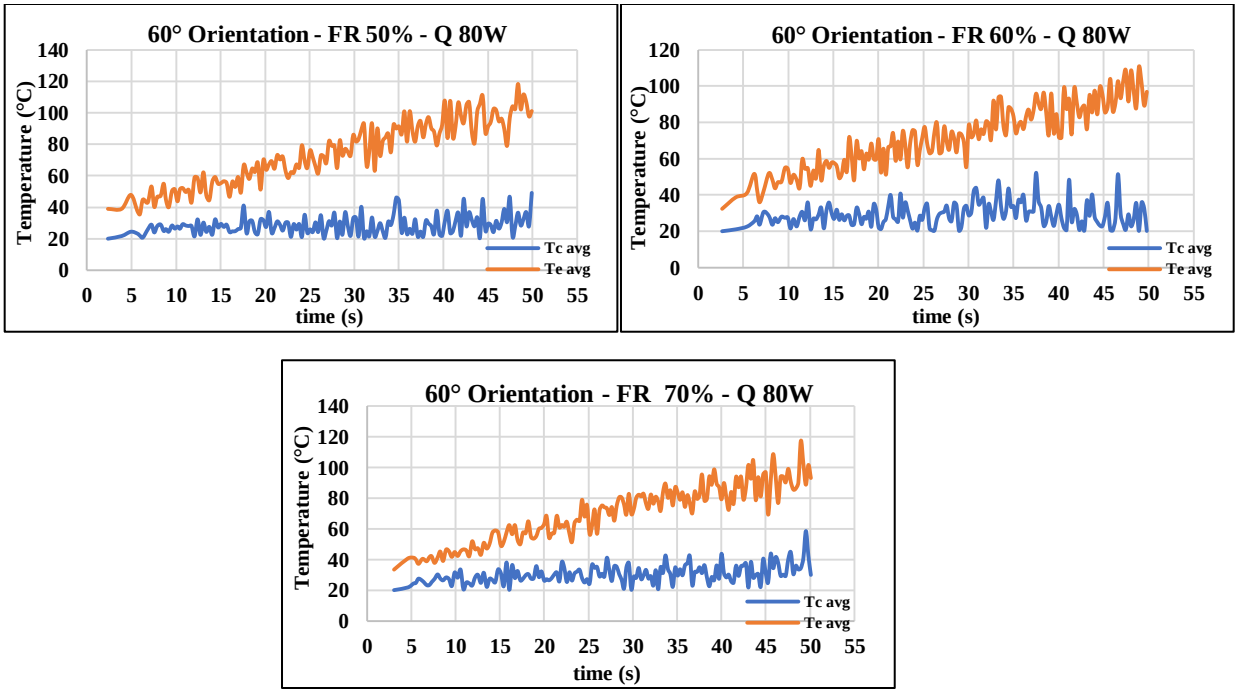

Figure 19: Numerically temperature variation in 60°orientation, for different charging ratios at 80 W heat-load after reaches steady-condition.

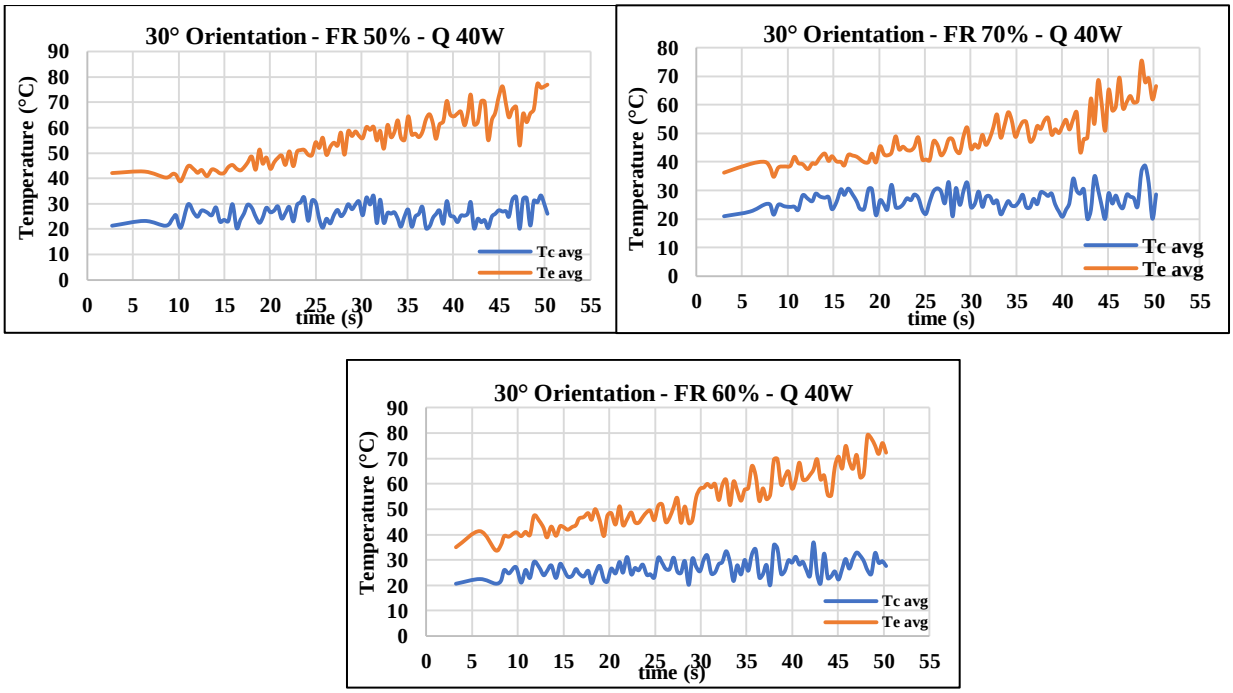

Figure 20: Numerically temperature variation in 30°orientation, for different charging ratios at 40 W heat-load after reaches steady-condition.

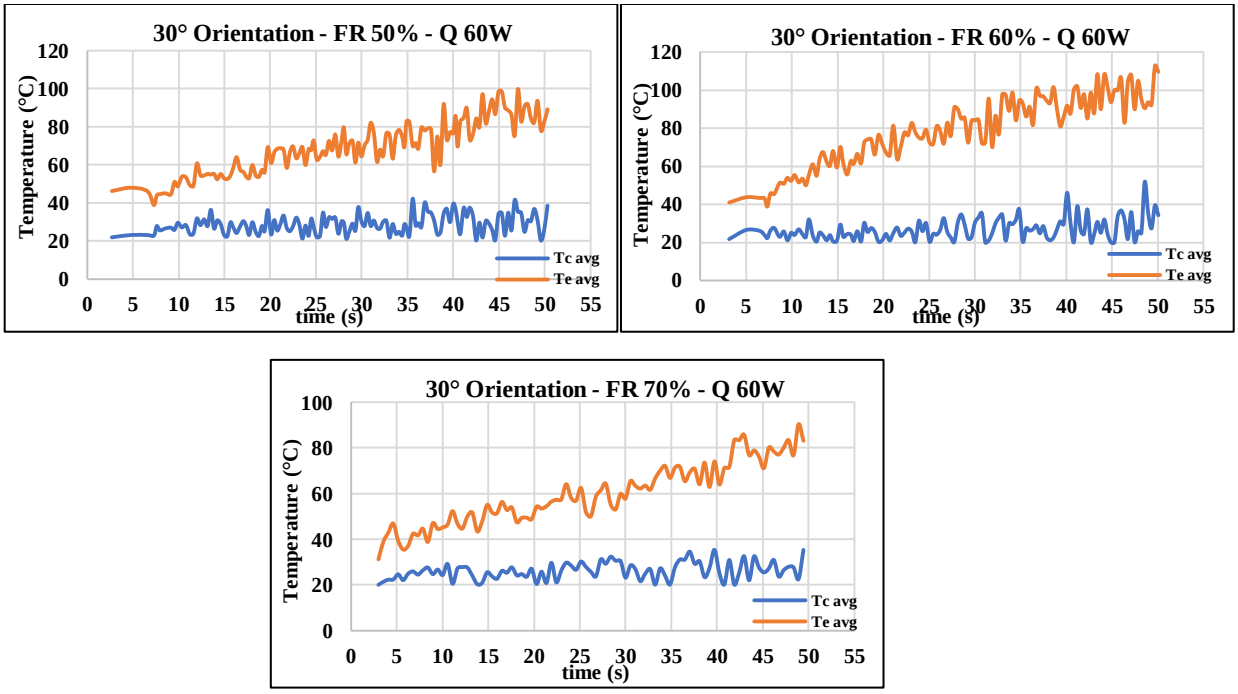

Figure 21: Numerically temperature variation in 30°orientation, for different charging ratios at 60 W heat-load after reaches steady-condition.

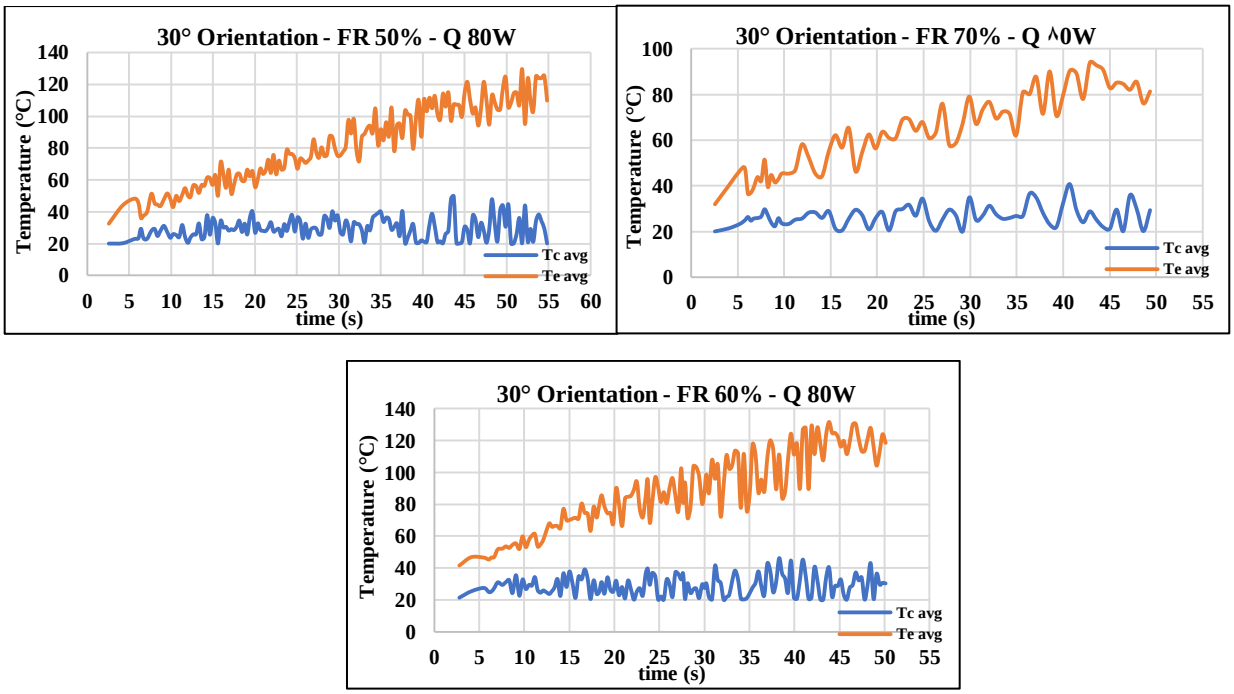

Figure 22: Numerically temperature variation in 30°orientation, for different charging ratios at 80 W heat-load after reaches steady-condition

5. Conclusions

To elucidate the influence of key operating parameters on the performance of oscillating heat-pipes, a comprehensive investigation was undertaken, employing both numerical and experimental methodologies.

The amplitude variations of the temperature of evaporator raised with the raising of heating power. The curves for the higher heat inputs (60 and 80 watts) appear to have higher average evaporator temperatures throughout the test compared to the 40-watt curve. The onset of oscillation occurs more rapidly with increasing input heat flux values compared to lower heat input conditions. Oscillation movement in tubes is proportional to charge ratio, and it is observed that it rises as charge ratio increases. It demonstrates that in CL-OHP, a sufficient charge ratio is required to maintain the motion of oscillation.

References

[1] D. J. Kearney, O. Suleman, J. Griffin, and G. Mavrakis, "Thermal performance of a PCB embedded pulsating heat pipe for power electronics applications," *Applied Thermal Engineering*, vol. 98, pp. 798-809, 2016.
doi: https://doi.org/10.1016/j.applthermaleng.2015.11.123

[2] C. Dang, L. Jia, and Q. Lu, "Investigation on thermal design of a rack with the pulsating heat pipe for cooling CPUs," *Applied Thermal Engineering*, vol. 110, pp. 390-398, 2017.
doi: https://doi.org/10.1016/j.applthermaleng.2016.08.187

[3] B. Agostini, M. Fabbri, J. E. Park, L. Wojtan, J. R. Thome, and B. Michel, "State of the art of high heat flux cooling technologies," *Heat transfer engineering*, vol. 28, no. 4, pp. 258-281, 2007.
doi: https://doi.org/10.1080/01457630601117799

[4] J. A. Olivier, J. B. Marcinichen, A. Bruch, and J. Thome, "Green cooling of high performance microprocessors: Parametric study between flow boiling and water cooling," 2011.
doi: https://doi.org/10.1115/1.4004435

[5] K. Roth, D. Westphalen, J. Dieckmann, S. Hamilton, and W. Goetzler, "Energy Consumption Characteristics of Commercial Building HVAC Systems, v. III: Energy Savings Potential," *Report for Building Technologies Program, Cambridge, MA*, 2002.

[6] G. Grover, T. Cotter, and G. Erickson, "Structures of very high thermal conductance," *Journal of applied physics*, vol. 35, no. 6, pp. 1990-1991, 1964.
doi: https://doi.org/10.1063/1.1713792

[7] H. Akachi, "Structure of heat pipe," *United States patent, Patent No. 4921041*, 1990.

[8] J. Qu, H. Wu, and P. Cheng, "Start-up, heat transfer and flow characteristics of silicon-based micro pulsating heat pipes," *International Journal of Heat and Mass Transfer*, vol. 55, no. 21-22, pp. 6109-6120, 2012.
doi:https://doi.org/10.1016/j.ijheatmasstransfer.2012.06.024

[9] J. Zhao, W. Jiang, and Z. Rao, "Thermal performance investigation of an oscillating heat pipe with external

expansion structure used for thermal energy recovery and storage," *International Journal of Heat and Mass Transfer*, vol. 132, pp. 920-928, 2019/04/01/ 2019, doi:https://doi.org/10.1016/j.ijheatmasstransfer.2018.12.084.

[10] H. Jin, G. Lin, A. Zeiny, L. Bai, J. Cai, and D. Wen, "Experimental study of transparent oscillating heat pipes filled with solar absorptive nanofluids," *International Journal of Heat and Mass Transfer*, vol. 139, pp. 789-801, 2019/08/01/ 2019, doi:https://doi.org/10.1016/j.ijheatmasstransfer.2019.04.117.

[11] H. Wang, J. Qu, Y. Peng, and Q. Sun, "Heat transfer performance of a novel tubular oscillating heat pipe with sintered copper particles inside flat-plate evaporator and high-power LED heat sink application," *Energy Conversion and Management*, vol. 189, pp. 215-222, 2019/06/01/ 2019, doi: https://doi.org/10.1016/j.enconman.2019.03.093.

[12] A. Wei, J. Qu, H. Qiu, C. Wang, and G. Cao, "Heat transfer characteristics of plug-in oscillating heat pipe with binary-fluid mixtures for electric vehicle battery thermal management," *International Journal of Heat and Mass Transfer*, vol. 135, pp. 746-760, 2019/06/01/ 2019, doi:https://doi.org/10.1016/j.ijheatmasstransfer.2019.02.021.

[13] H. Jafari Mosleh, M. A. Bijarchi, and M. B. Shafii, "Experimental and numerical investigation of using pulsating heat pipes instead of fins in air-cooled heat exchangers," *Energy Conversion and Management*, vol. 181, pp. 653-662, 2019/02/01/ 2019, doi: https://doi.org/10.1016/j.enconman.2018.11.081.

[14] J. Liu, F. Shang, K. Yang, C. Liu, and Y. Wu, "Study on application technology of pulsating heat pipe," in *E3S Web of Conferences*, 2021, vol. 248: EDP Sciences, p. 01051.doi: https://doi.org/10.1051/e3sconf/202124801051

[15] Y. Hai, *Experiment of Thermal Performance of Oscillating Heat Pipe Under Various Conditions*. University of California, Irvine, 2020.

[16] S. Khandekar and M. Groll, "An insight into thermo-hydrodynamic coupling in closed loop pulsating heat pipes," *International Journal of Thermal Sciences*, vol. 43, no. 1, pp. 13-20, 2004/01/01/ 2004, doi: https://doi.org/10.1016/S1290-0729(03)00100-5.

[17] D. Bastakoti, H. Zhang, D. Li, W. Cai, and F. Li, "An overview on the developing trend of pulsating heat pipe and its performance," *Applied Thermal Engineering*, vol. 141, pp. 305-332, 2018/08/01/ 2018, doi:https://doi.org/10.1016/j.applthermaleng.2018.05.121.

[18] H. Xian, Y. Yang, D. Liu, and X. Du, "Heat Transfer Characteristics of Oscillating Heat Pipe With Water and Ethanol as Working Fluids," *Journal of Heat Transfer*, vol. 132, no. 12, 2010, doi: https://doi.org/10.1115/1.4002366.

[19] Y. Ji, H.-h. Chen, Y. J. Kim, Q. Yu, X. Ma, and H. B. Ma, "Hydrophobic Surface Effect on Heat Transfer Performance in an Oscillating Heat Pipe," *Journal of Heat Transfer*, vol. 134, no. 7, 2012, doi: https://doi.org/10.1115/1.4006111.

[20] Z. Lin, S. Wang, J. Chen, J. Huo, Y. Hu, and W. Zhang, "Experimental study on effective range of miniature oscillating heat pipes," *Applied Thermal Engineering*, vol. 31, no. 5, pp. 880-886, 2011/04/01/ 2011, doi: https://doi.org/10.1016/j.applthermaleng.2010.11.009.

[21] K.-H. Chien, Y.-T. Lin, Y.-R. Chen, K.-S. Yang, and C.-C. Wang, "A novel design of pulsating heat pipe with fewer turns applicable to all orientations," *International Journal of Heat and Mass Transfer*, vol. 55, no. 21, pp. 5722-5728, 2012/10/01/ 2012, doi: https://doi.org/10.1016/j.ijheatmasstransfer.2012.05.068.

[22] V. M. Patel, Gaurav, and H. B. Mehta, "Influence of working fluids on startup mechanism and thermal performance of a closed loop pulsating heat pipe," *Applied Thermal Engineering*, vol. 110, pp. 1568-1577, 2017/01/05/ 2017, doi: https://doi.org/10.1016/j.applthermaleng.2016.09.017.

[23] V. S. Nikolayev, "Effect of tube heat conduction on the single branch pulsating heat pipe start-up," *International Journal of Heat and Mass Transfer*, vol. 95, pp. 477-487, 2016/04/01/ 2016, doi: https://doi.org/10.1016/j.ijheatmasstransfer.2015.12.016.

[24] I. Nekrashevych and V. S. Nikolayev, "Effect of tube heat conduction on the pulsating heat pipe start-up," *Applied Thermal Engineering*, vol. 117, pp. 24-29, 2017/05/05/ 2017, doi: https://doi.org/10.1016/j.applthermaleng.2017.02.013.

[25] Y. Xu, Y. Xue, H. Qi, and W. Cai, "Experimental study on heat transfer performance of pulsating heat pipes with hybrid working fluids," *International Journal of Heat and Mass Transfer*, vol. 157, p. 119727, 2020. doi: https://doi.org/10.1016/j.ijheatmasstransfer.2020.119727

[26] A. S. Barrak, A. A. Saleh, and Z. H. Naji, "An experimental study of using water, methanol, and binary fluids in oscillating heat pipe heat exchanger," *Engineering Science and Technology, an International Journal*, vol. 23, no. 2, pp. 357-364, 2020, doi: https://doi.org/10.1016/j.jestch.2019.05.010

[27] J. Qu, A. Zuo, F. Liu, and Z. Rao, "Quantitative analysis of thermal performance and flow characteristics of oscillating heat pipes with different initial pressure," *Applied Thermal Engineering*, vol. 181, p. 115962, 2020. doi: https://doi.org/10.1016/j.applthermaleng.2020.115962

[28] K. Mehta, N. Mehta, and V. Patel, "Experimental investigation of the thermal performance of closed loop flat plate oscillating heat pipe," *Experimental Heat Transfer*, vol. 34, no. 1, pp. 85-103, 2021. doi: https://doi.org/10.1080/08916152.2020.1718802

[29] N. Kammuang-lue, P. Sakulchangsatjatai, and P. Terdtoon, "Thermal performance of various adiabatic section lengths of closed-loop pulsating heat pipe

designed for energy recovery applications," *Energy Reports*, vol. 8, pp. 731-737, 2022.
doi: https://doi.org/10.1016/j.egyr.2022.10.149

[30] Q. Li, C. Wang, Y. Wang, Z. Wang, H. Li, and C. Lian, "Study on the effect of the adiabatic section parameters on the performance of pulsating heat pipes," *Applied Thermal Engineering*, vol. 180, p. 115813, 2020.
doi:https://doi.org/10.1016/j.applthermaleng.2020.115813

[31] M. Siritan, N. Kammuang-Lue, P. Terdtoon, and P. Sakulchangsatjatai, "Thermal performance and thermo-economics analysis of evacuated glass tube solar water heater with closed-loop pulsating heat pipe," *Case Studies in Thermal Engineering*, vol. 35, p. 102139, 2022.
doi: https://doi.org/10.1016/j.csite.2022.102139

[32] S. Hammad, "Design and Investigation of a pulsating heat pipe for electronic cooling," Lund University, 2023.
doi: http://lup.lub.lu.se/student-papers/record/9133930

[33] J. Choi and Y. Zhang, "Numerical simulation of oscillatory flow and heat transfer in pulsating heat pipes with multi-turns using OpenFOAM," *Numerical Heat Transfer, Part A: Applications*, vol. 77, no. 8, pp. 761-781, 2020.
doi: https://doi.org/10.1080/10407782.2020.1717202

[34] D.-T. Vo, H.-T. Kim, J. Ko, and K.-H. Bang, "An experiment and three-dimensional numerical simulation of pulsating heat pipes," *International Journal of Heat and Mass Transfer*, vol. 150, p. 119317, 2020.
doi:https://doi.org/10.1016/j.ijheatmasstransfer.2020.119317

[35] W.-W. Wang *et al.*, "Thermo-hydrodynamic model and parametric optimization of a novel miniature closed oscillating heat pipe with periodic expansion-constriction condensers," *International Journal of Heat and Mass Transfer*, vol. 152, p. 119460, 2020.
doi:https://doi.org/10.1016/j.ijheatmasstransfer.2020.119460